

Converter Design for Electrolytic capacitor-less Two Stage PV System

*Report submitted in fulfillment of the requirements
for the Undergraduate Project of*

Fourth Year B.Tech.

by

Atul Kumar, L N Saaswath, Aadhar Srivastava

Under the guidance of

Dr V N Lal



Department of Electrical Engineering

INDIAN INSTITUTE OF TECHNOLOGY (BHU) VARANASI

Varanasi 221005, India

December 2022

Declaration

I certify that

1. The work contained in this report is original and has been done by myself and the general supervision of my supervisor.
2. The work has not been submitted for any project.
3. Whenever I have used materials (data, theoretical analysis, results) from other sources, I have given due credit to them by citing them in the text of the thesis and giving their details in the references.
4. Whenever I have quoted written materials from other sources, I have put them under quotation marks and given due credit to the sources by citing them and giving required details in the references.

Place: IIT (BHU) Varanasi
Date:

Atul Kumar, L N Saaswath, Aadhar Srivastava
IDD Students
Department of Electrical Engineering,
Indian Institute of Technology (BHU) Varanasi,
Varanasi, INDIA 221005.

Certificate

*This is to certify that the work contained in this report entitled “**Converter Design for Electrolytic capacitor-less Two Stage PV System**” being submitted by **Atul Kumar, L N Saaswath, Aadhar Srivastava (Roll No. 19084007, 19084011, 19084001)**, carried out in the Department of Computer Science and Engineering, Indian Institute of Technology (BHU) Varanasi, is a bona fide work of our supervision.*

Place: IIT (BHU) Varanasi
Date:

Dr V N Lal
Department of Computer Science and Engineering,
Indian Institute of Technology (BHU) Varanasi,
Varanasi, INDIA 221005.

Acknowledgments

We express our sincere gratitude to Dr V N Lal for allowing us to work on this project in VLPERI Lab. We are truly grateful to Mr Aman Yaduvanshi and Mr Prakash Ji Barnawal for the motivation, support, and guidance they have given us throughout the project.

Place: IIT (BHU) Varanasi

Date: **Atul Kumar, L N Saaswath, Aadhar Srivastava**

Abstract

An intermediate dc-link electrolytic capacitor, which is used in three-phase inverters in electric vehicles, hybrid electric vehicles, and uninterrupted power supplies, has reliability concerns and is a common reason for inverter failure and short lifespan. The size and price of the system are increased by the electrolytic capacitor's high capacity. This problem has recently been addressed in research on electrolytic capacitor-less inverters employing the six-pulse modulation approach and high-frequency power conversion. Due to the lack of a capacitor in the dc-link, closed-loop operation and control have some limitations. The electrolytic capacitor-less six-pulse DC Link three-phase inverter's closed-loop functioning, design, and implementation are discussed in this work involving dual-bridge converter and film capacitor.

Contents

List of Figures	ix
1 Introduction	1
1.1 Overview	1
1.2 Motivation of the Research Work	2
2 Dual Bridge Converter	3
2.1 Dual Active Bridge Converter	3
2.2 Applications	4
2.3 Operation of DAB	4
3 Theory of Operation	6
3.1 Six Pulse Modulation (SPM)	6
3.2 Operation	9
3.3 Closed Loop control (PI controller for stage 1)	12
4 Design and Simulation of Converter	14
4.1 Power Converter Design	15
4.2 Open-Loop Design and Simulation	16
4.3 Closed Loop Control	17
5 Conclusion	22

Bibliography	24
--------------	----

List of Figures

1.1	Conventional PV Two Grid System	2
2.1	Schematic of Dual Active Bridge Converter	4
3.1	Schematic of the capacitor-less three phase inverter	6
3.2	Rectified three-phase sinusoidal signals creating six-pulse dc bus. . . .	7
3.3	Gating Signal (V_{gate}) generated by SPM with Modulating signal (V_{sin1}) and Carrier signal (V_{tri1})	8
3.4	Zoomed version of above Fig. 4.3	8
3.5	DC-Pulsating DC Stage, designed in PSIM	9
3.6	Primaries in DCM Operation	11
3.7	Primaries in BCM Operation	11
3.8	Stage two Inverter in PSIM	12
3.9	Block diagram of a system with PI controller	12
4.1	Open-loop PV Converter-Inverter System in PSIM	16
4.2	Control logic of Gating signals in Open-Loop (PWM, SOLM)	16
4.3	Gating Signal Generated through SPM with Modulation and Carrier Signals	17
4.4	Switching Timing Diagram, Primary Voltage, Primary Current in Open- loop BCM	17
4.5	DC Link Voltage and Inverter Output in Open-Loop	18

4.6	Rectified Six Pulse Voltage and Inverter waveforms(Reference)	19
4.7	Bode plot of control-to-output transfer function in open-loop	19
4.8	Simplified closed-loop block diagram of the dc to pulsating dc stage .	20
4.9	Closed-loop Converter Design in MATLAB	20
4.10	Pulsating DC Voltage output of closed-loop control in MATLAB . . .	21

Chapter 1

Introduction

1.1 Overview

Electrolytic capacitor-less inverter topologies eliminate the bulky dc bus capacitors entirely in order to increase reliability, reduce cost, and reduce system volume. For fuel cell or battery powered electric, hybrid electric cars, and uninterrupted power supply (UPS) systems, such power conversion devices have bright futures. Capacitor-less inverter designs and unique modulation methods have been developed to address these problems.

This project's objective is to present closed-loop analysis, design, and implementation in order to create and show the inverter's closed-loop performance and operation. To maintain the necessary amount of dc bus voltage and its distinctive six-pulse waveform, a proportional integral (PI) controller has been designed, developed, and put into practise. Performance evaluation has been done for various loading conditions up to 3.4 kW power level.

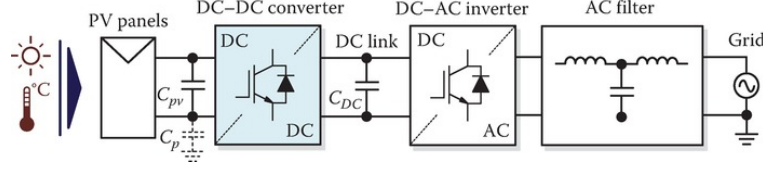


Figure 1.1 Conventional PV Two Grid System

1.2 Motivation of the Research Work

The literature has long discussed intermediate dc-link-based inverter methods. To create a constant dc-link (V_{dc}) and to eliminate the harmonic pulsation of a three-phase ac output, they use electrolytic capacitor(s). The electrolytic capacitor is expensive, unreliable, and has a big volume. Aluminum electrolytic capacitors convince with high specific energy densities and foil capacitors offer great ripple current capability. But their lifespan varies between 1-2 years whereas an average inverter lasts for 7-8 years. They face ageing effect, dry-out and require continuous monitoring and protection. Hence we introduce electrolytic capacitor-less topology to tackle the issues cause by the heavy electrolytic capacitors.

To overcome these issues, capacitor-less inverter topologies along with special modulation techniques have come up [1], [2]. However, amongst multiple capacitor-less topologies, the topology and modulation method presented in [3], [4], [5] have the advantages of lesser number of semiconductor switches, one single-phase high-frequency (HF) transformer, reduced gate-drive and control circuit, lower switching loss at three-phase inverter side, and reduced magnetics.

This work discusses the need for electrolytic capacitor-less topologies and focusses on bringing efficient closed-loop control to such topologies as previous works have well worked on open loop and other modulation techniques.

The available literature for such modulation techniques for capacitorless inverter topologies is only on steady-state analysis and performance. However, closed-loop analysis, design, and performance have not been investigated until recent years[6].

Chapter 2

Dual Bridge Converter

In this chapter, we discuss the theory of the dual active bridge converter - its application, operation and how it is used in the converter design in our research.

2.1 Dual Active Bridge Converter

The single-phase Dual Active Bridge (DAB) converter is a highly efficient isolated bidirectional DC-to-DC converter. Its key features are:

- Isolated operation; reliability is high.
- Power density (high-frequency operation reduces the size of the isolation transformer)
- Bidirectional power flow
- Efficiency is high(Zero Voltage Switching)
- Weightless; and size is compact.

2.2 Applications

It is used in several applications such as in charging stations, electric vehicle traction, automotive applications[7] [5]. Vehicle-to-Grid (V2G) systems are also using this type of converters[8].

2.3 Operation of DAB

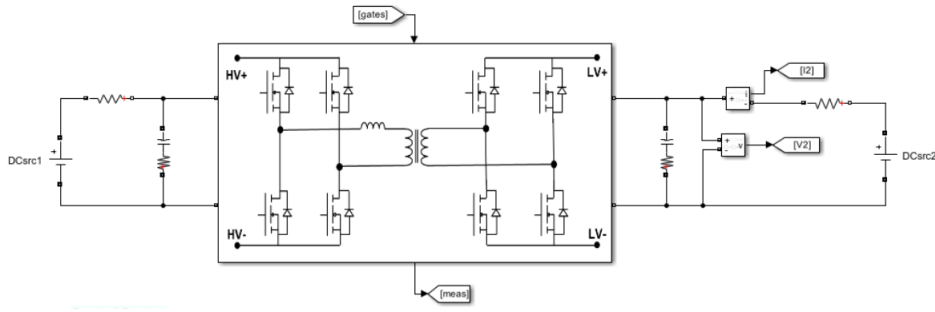


Figure 2.1 Schematic of Dual Active Bridge Converter

The two legs of both full-bridges are driven with complimentary square-wave pulses. Power flow in the dual active bridge can be directed by phase-shifting the pulses of one bridge with respect to the other using phase shift modulation. The control directs power between the two DC buses such that the leading bridge delivers power to the lagging bridge. The applied square waves to the bridges create a voltage differential across the energy transfer inductance and direct its stored energy. In ideal cases with dual active bridge converters, zero voltage switching (ZVS) can be realized when the voltage transfer ratio (M) across the transformer is equal to 1:

$$M = \frac{V_{out}}{n * V_{in}}$$

where, n is the transformer turn ratio, V_{out} is the output voltage and V_{in} is the

2.3. Operation of DAB

input voltage. In non-ideal cases, ZVS depends on the resonant relationship between the output capacitance across each device and the equivalent inductance of the circuit during different switching intervals.

During switching events, the current through one of the complementary devices is interrupted, but due to the energy transfer inductance, current is supplied through the output capacitor and forced through the anti-parallel diode of the device.

In our work the dual-active bridge converter is used as a dual bridge converter which is made possible with H-bridge inverter, diode rectifier and film capacitor as DC Link for pulsating DC voltage.

Chapter 3

Theory of Operation

In this chapter, we discuss the brief of the theory of operation, of both the stages of the designed circuit, with focus over the stage one converter design.

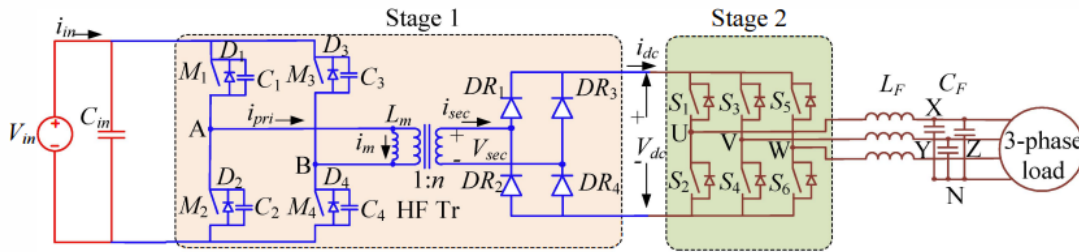


Figure 3.1 Schematic of the capacitor-less three phase inverter

3.1 Six Pulse Modulation (SPM)

This project proposes a hybrid modulation technique that comprises two different modulations for the two stages. Single Reference Six Pulse Modulation (SRSPM) is proposed to control front-end full-bridge dc/dc converter to produce HF pulsating dc voltage having six-pulse information on an average. A single reference signal is used for SRSPM implementation. Second modulation is 33% (or one third) modulation adopted for a three-phase inverter that produces balanced three-phase voltage. In 33% modulation, only one leg is modulated at a time. It reduces the average

3.1. Six Pulse Modulation (SPM)

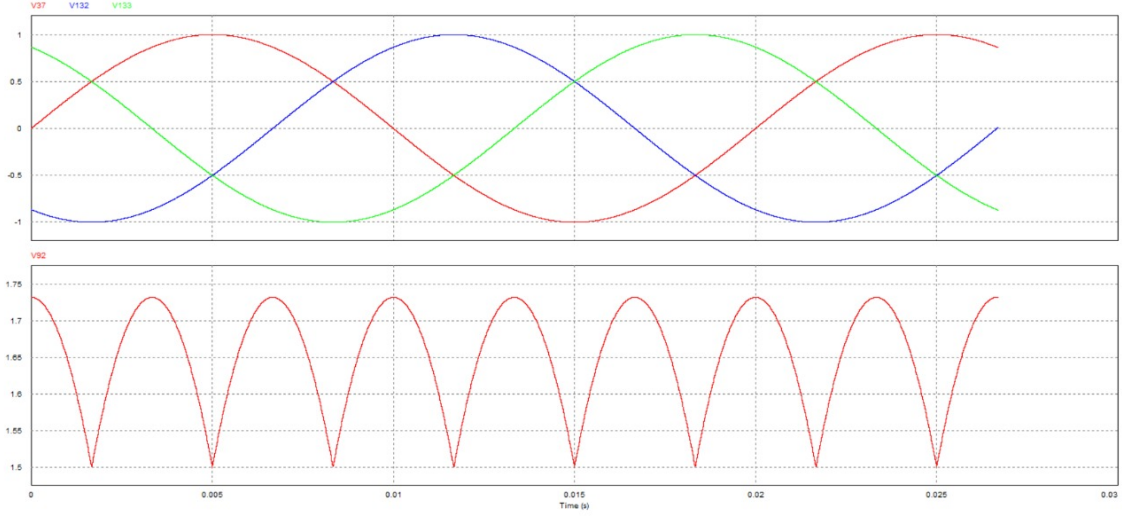


Figure 3.2 Rectified three-phase sinusoidal signals creating six-pulse dc bus.

switching frequency and limits the switching losses to 33% of the conventional value. Interleaving does not affect the modulation implementation, or in other words the proposed SRSPM is applicable to single full-bridge unit too.

The overall system has the following merits:

- 1) Elimination of dc-link electrolytic capacitor: reduces volume of system and improves reliability;

- 2) Reduced average switching frequency of inverter: at any instant of time, only one leg of inverter is modulated at HF keeping other two legs at same switching state. This reduces the switching losses and improves efficiency. Switching losses are further reduced because the devices are not commutated when current is at its peak.

- 3) Single reference front-end modulation: A single reference signal is used to implement six-pulse modulation to produce pulsating dc voltage at the dc link.

The H-bridge is modulated using identical six-pulse modulation producing HF pulsating dc voltage V_{dc} , fed to a standard three-phase inverter.

3.1. Six Pulse Modulation (SPM)

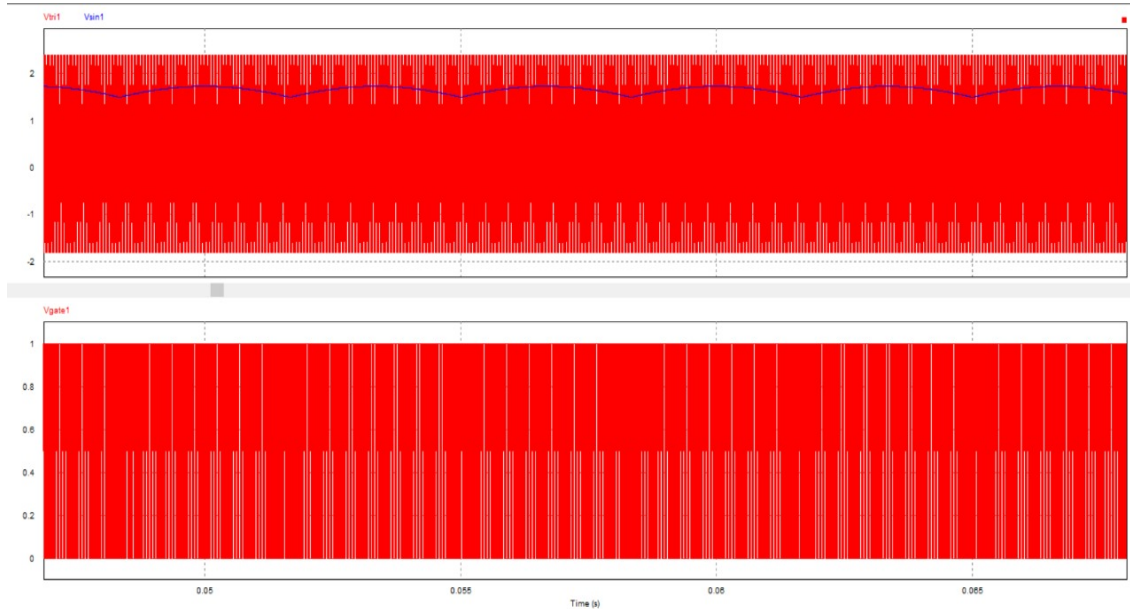


Figure 3.3 Gating Signal (V_{gate}) generated by SPM with Modulating signal (V_{sin1}) and Carrier signal (V_{tri1})

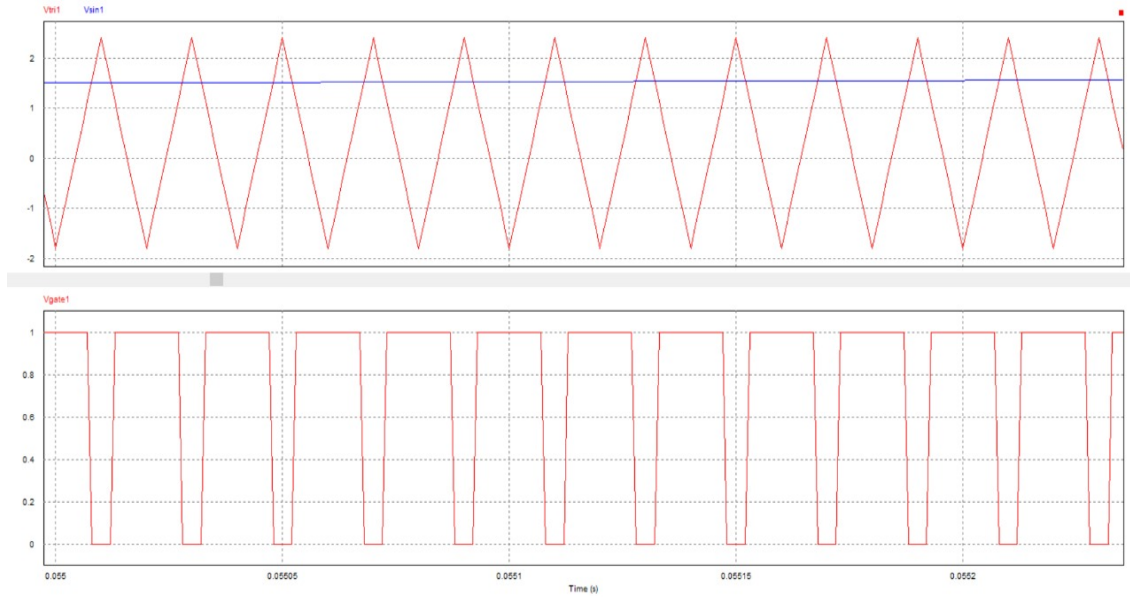


Figure 3.4 Zoomed version of above Fig. 4.3

3.2. Operation

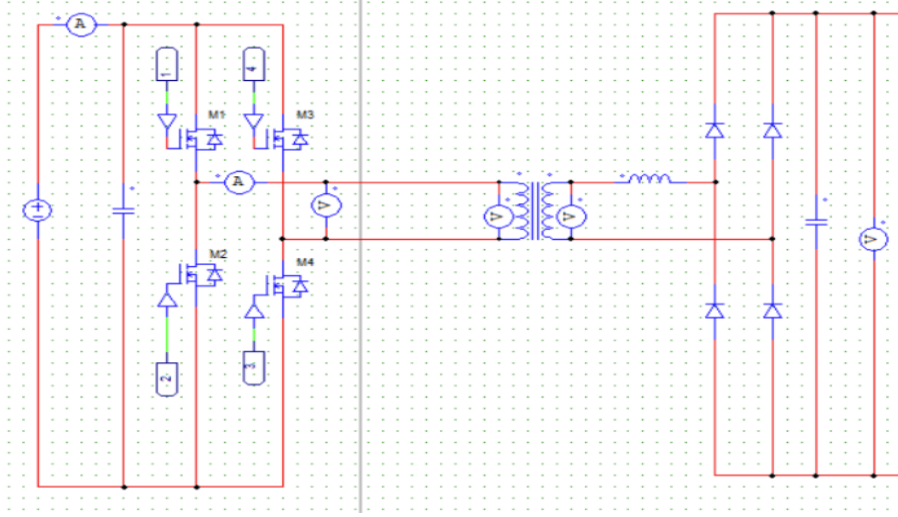


Figure 3.5 DC-Pulsating DC Stage, designed in PSIM

3.2 Operation

The system consists of two stages of power conversion:

1. dc to pulsating dc conversion stage (Stage1 as shown in Figure 4.1)
2. pulsating dc to three-phase ac inverter stage.

DC to pulsating DC stage using SPM

The input for this converter is a low voltage dc source (V_{in}), as shown. The first aim is to convert V_{in} into a pulsating dc voltage V_{dc} , which resembles a six-pulse rectified waveform. If a three-phase balanced sinusoidal voltage (V_a , V_b , V_c) is rectified by a three-phase diode-bridge rectifier without a dc bus capacitor, then the dc bus voltage waveform is similar to V_{6p} , as shown in Figure 4.2.

It comprises six segments or pulses from the three-line voltage within a line cycle. Such a six-pulse waveform, V_{6p} , can be created inside a digital controller. To generate a six-pulse dc bus in the power converter, an H-bridge converter is used in Stage1 to convert V_{in} into HF quasi-square wave ac voltage (V_{pri}) at the primary of HF

transformer[5]. The gating signals for the H-bridge inverter can be generated by taking V_{6p} as a modulating signal and comparing it with triangular carrier wave V_c under open-loop conditions[1]. Fig. 4.5 depicts the design of this stage in PSIM.

The average value of V_{gate} taken over each switching period would also have a six-pulse profile. The pulse width of V_{gate} is the period for which a voltage, V_{pri} , is to be applied on the primary of the HF transformer. The gating signals (GM1, GM2, GM3, and GM4) for the top and bottom switches of leg A and leg B, as shown in the figure, of the H-bridge are complimentary with a deadband. Next, V_{pri} is amplified by the HF transformer to the required voltage level by turns ratio “n” of the transformer at the secondary side (V_{sec}), as shown in Fig. 1. Finally, V_{sec} is rectified by a single-phase diode-bridge rectifier. The average value of pulsating dc voltage output in each HF cycle is obtained as-

$$V_{dc} = 2D.n.V_{in}$$

Here, D(Duty ratio) varies at each cycle.

Conduction Modes - BCM and DCM

The H-bridge switches are chosen as MOSFETs and they are represented by the symbols M1 , M2 , M3 , and M4 , as shown. The body diodes of the MOSFETs are labeled as D1 , D2 , D3 , and D4 . When the gating signals GM1 and GM4 are high then a positive voltage is applied across the transformer primary and a current (I_{pri}) with positive slope starts flowing through the winding.

Next, GM1 is turned OFF which makes the positive current shifted to diode D2. When GM2 and GM4 are high, then the current I_{pri} freewheels through D2 ,M4 , and transformer primary. The slope of current is negative and decided by reflected secondary voltage and leakage inductance. Depending on loading, two cases are

3.2. Operation

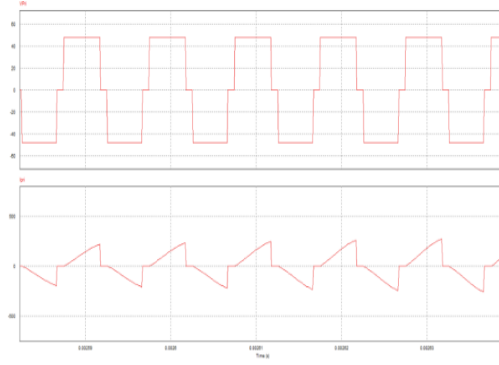


Figure 3.6 Primaries in DCM Operation

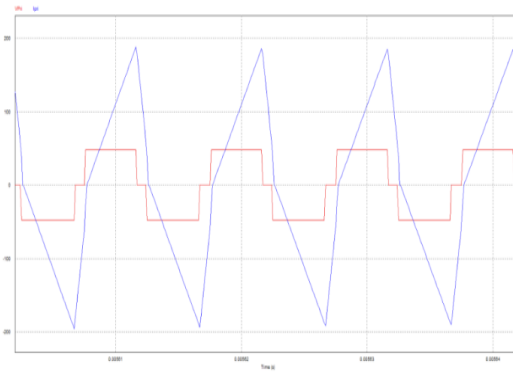


Figure 3.7 Primaries in BCM Operation

possible.

a) Case 1: If the current reaches zero before GM4 to GM2 transition then ideally primary current stays at zero and this is DCM operation. When GM4 is switched OFF, the turn-off occurs at zero current. Fig 4.6 depicts the output of primary voltage and primary current in DCM operation.

b) Case 2: If the current remains positive when GM4 to GM2 transition occurs, then across the leakage inductance, reflected secondary and primary voltage is applied and with an increased negative slope the current is reversed. In this process, current becomes zero at one instant only and this situation can be termed as BCM. Fig 4.7 depicts the output of primary voltage and primary current in BCM operation.

3.3. Closed Loop control (PI controller for stage 1)

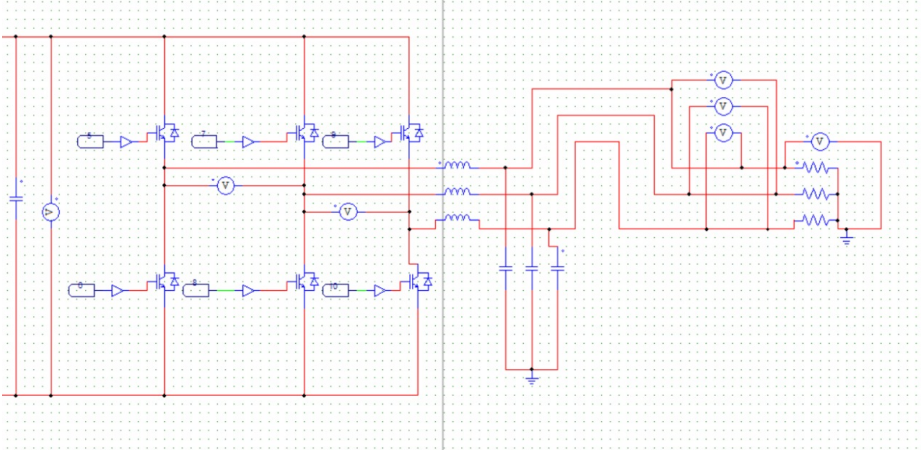


Figure 3.8 Stage two Inverter in PSIM

Pulsating DC Stage to Three-Phase AC Using SOLM

Inverter is used to convert pulsating DC to three-phase AC using SOLM(synchronous one leg modulation) by synchronously switching the three-phase inverter devices[6].

In this project we use H-bridge inverter in the dual bridge converter of power stage, the design of inverter of stage two(Fig. 4.8) is not included.

3.3 Closed Loop control (PI controller for stage 1)

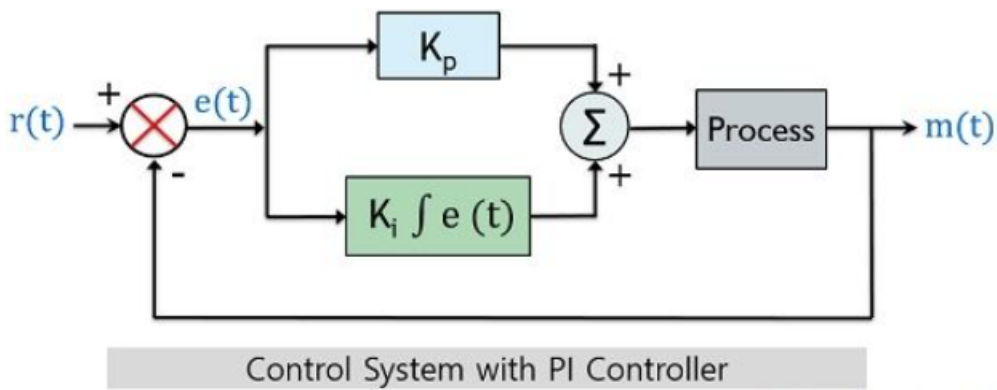


Figure 3.9 Block diagram of a system with PI controller

3.3. Closed Loop control (PI controller for stage 1)

Proportional Integral controller sometimes also known as proportional plus integral (PI) controllers. It is a type of controller formed by combining proportional and integral control action. Thus it is named as PI controller. In the proportional-integral controller, the control action of both proportional, as well as the integral controller, is utilized. This combination of two different controllers produces a more efficient controller which eliminates the disadvantages associated with each one of them. In this case, the control signal shows proportionality with both the error signal as well as with integral of the error signal. Mathematical representation of proportional plus integral controller is given as:

$$m(t) = K_p e(t) + K_i \int e(t)$$

Chapter 4

Design and Simulation of Converter

In this chapter, we discuss the design of the converter and inverter used to experiment and simulate the circuit. The experimental results and intermediate waveforms are also discussed. The closed control PI design of the dual-bridge converter is covered too.

4.1 Power Converter Design

Input voltage, $V_{in} = 48V$

Phase output voltage, $V_{out} = 241.34V$

Output frequency, $f_o = 50Hz$

Output power, $P_o = 3.14kW$

Switching frequency = $100kHz$

Switching frequency of three phase inverter = $10kHz$

Average input current, $I_{in} = 74.56A$.

Turns ratio of HF transformer, $n = 10$.

- Maximum value of average voltage at dc-link should be above peak value of line-line output voltage. $V_{dc} = 591.15V$
- Assuming an efficiency η of nearly 95%.

Operation of this conversion stage is similar to a DCM buck converter operation. Therefore, the input output relation can be rewritten as the gain equation below, considering that all the circuit parameters are reflected on the transformer secondary side. [9]

$$M = \frac{V_{dc}}{nV_{in}} = \frac{2}{1 + \sqrt{1 + \frac{8Lf_{sw}}{D_b^2 R}}}$$

4.2 Open-Loop Design and Simulation

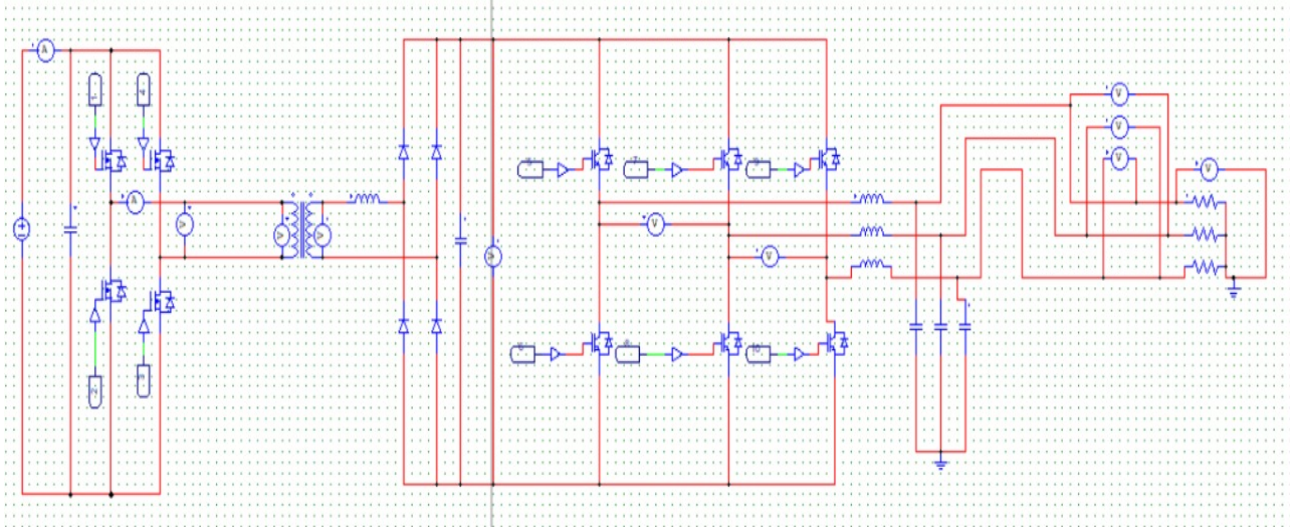


Figure 4.1 Open-loop PV Converter-Inverter System in PSIM

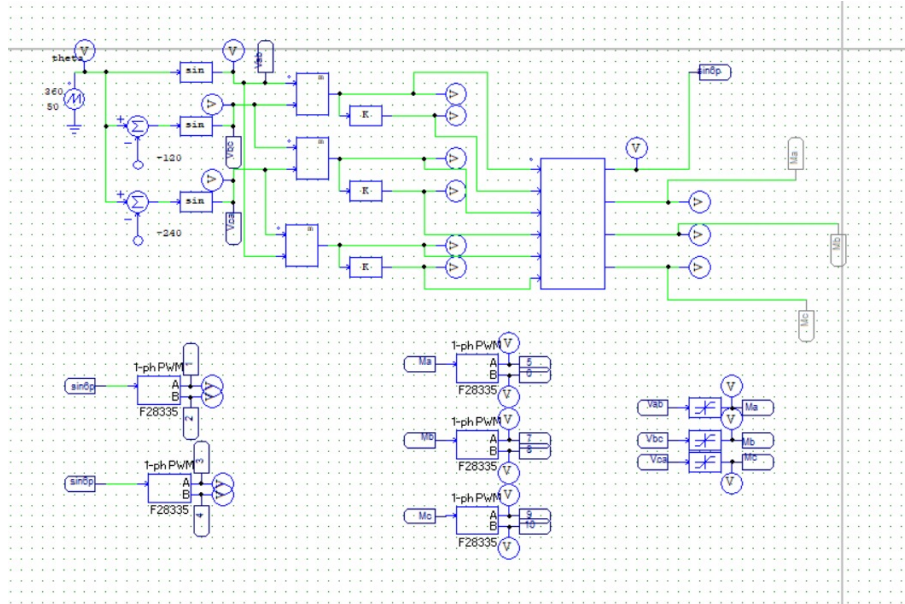


Figure 4.2 Control logic of Gating signals in Open-Loop (PWM, SOLM)

4.3. Closed Loop Control

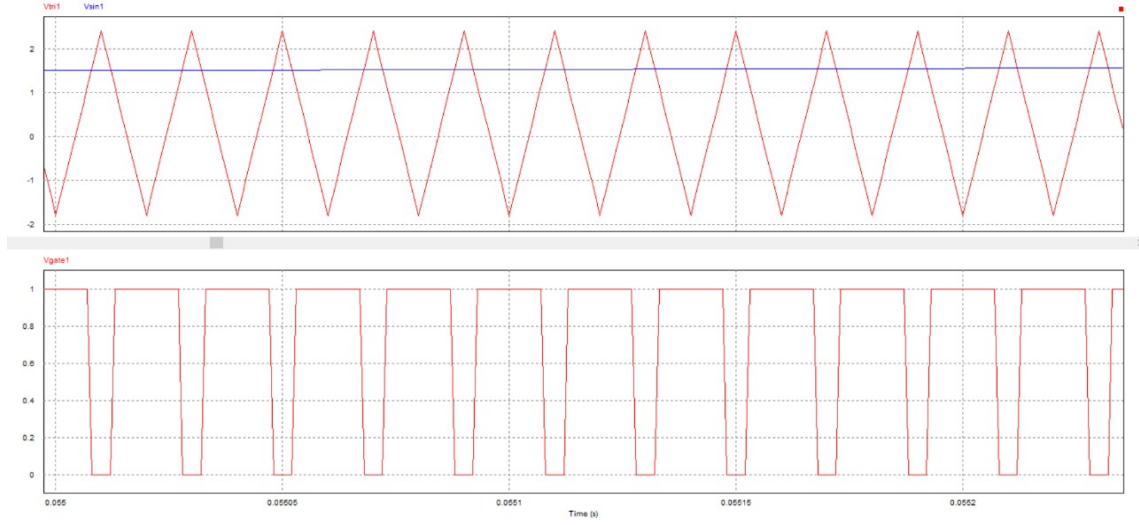


Figure 4.3 Gating Signal Generated through SPM with Modulation and Carrier Signals

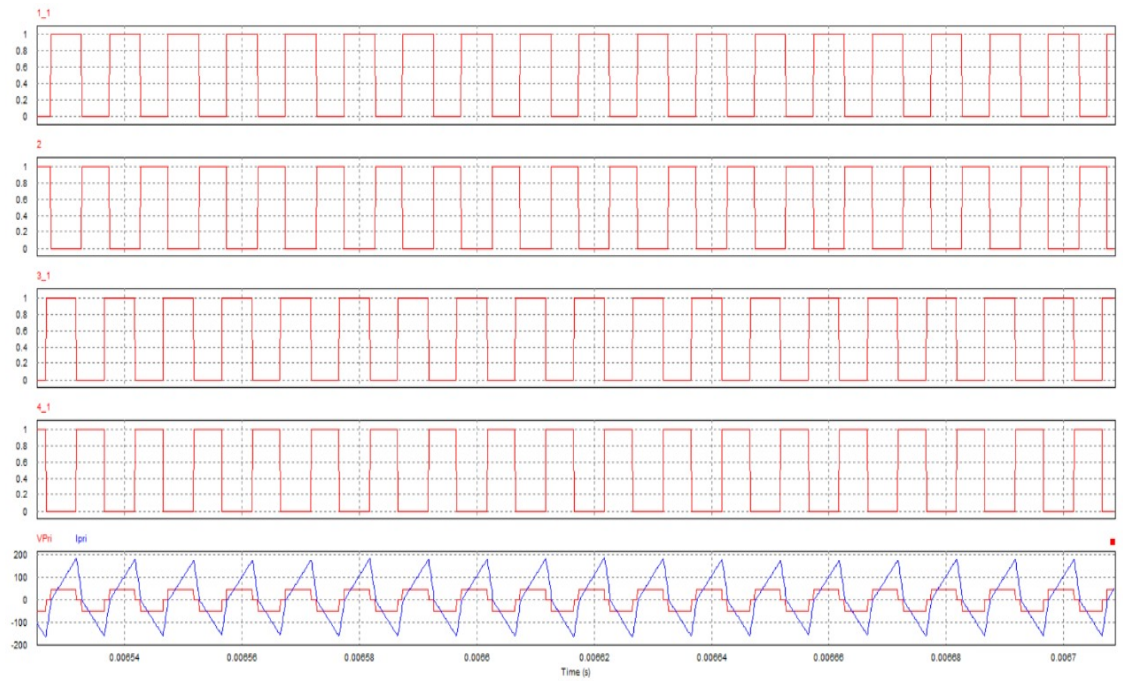


Figure 4.4 Switching Timing Diagram, Primary Voltage, Primary Current in Open-loop BCM

4.3 Closed Loop Control

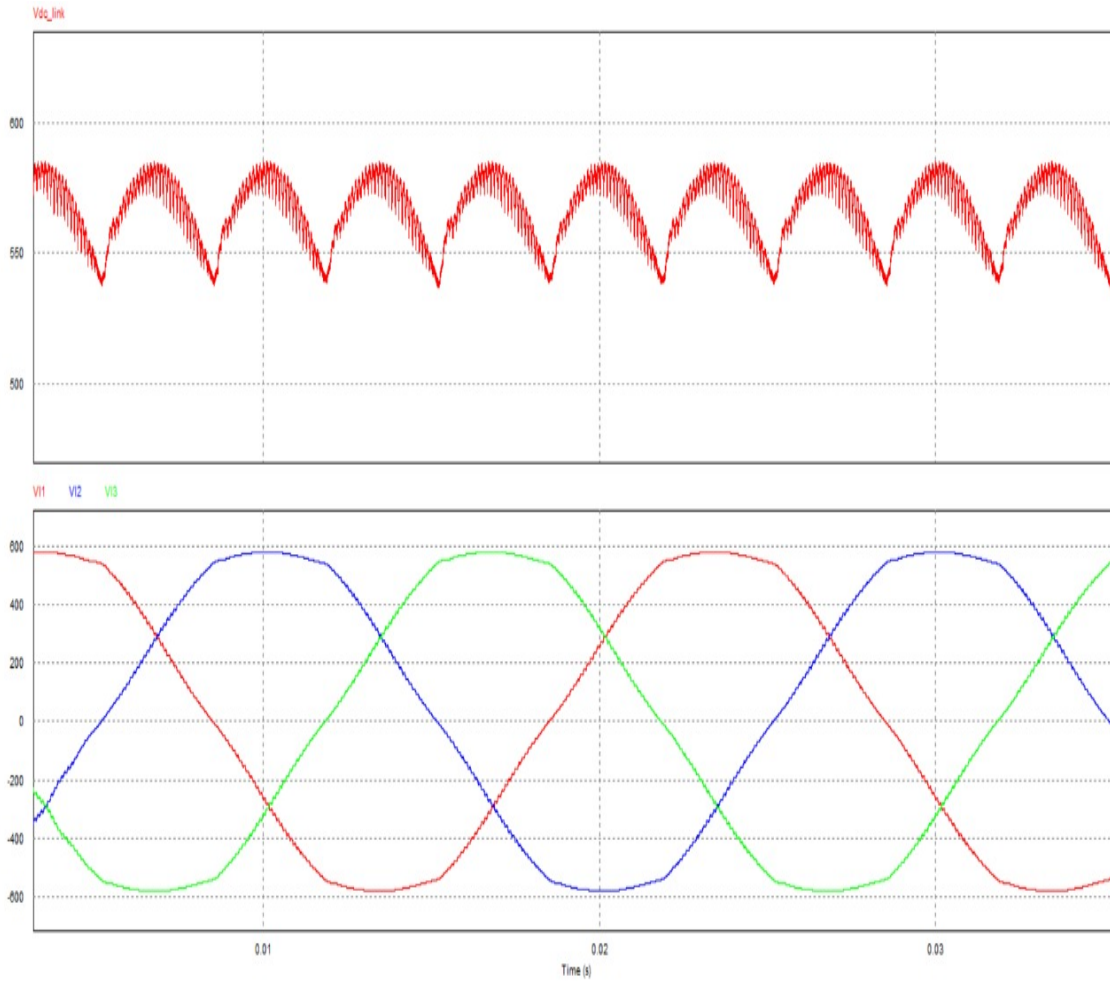


Figure 4.5 DC Link Voltage and Inverter Output in Open-Loop

4.3. Closed Loop Control

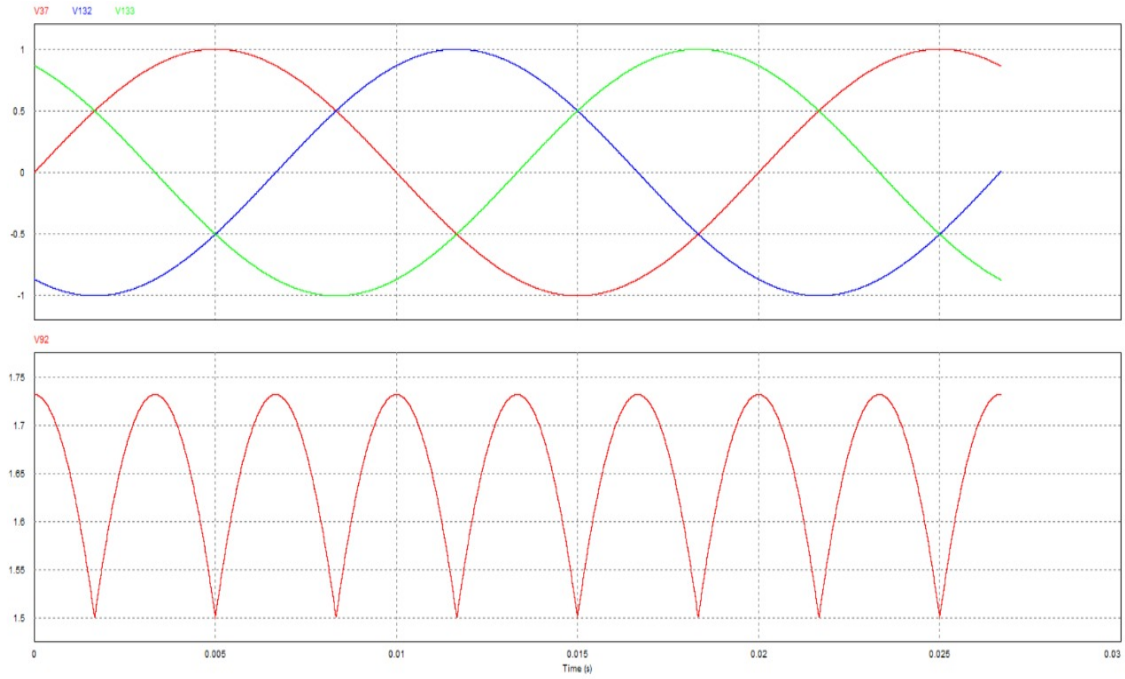


Figure 4.6 Rectified Six Pulse Voltage and Inverter waveforms(Reference)

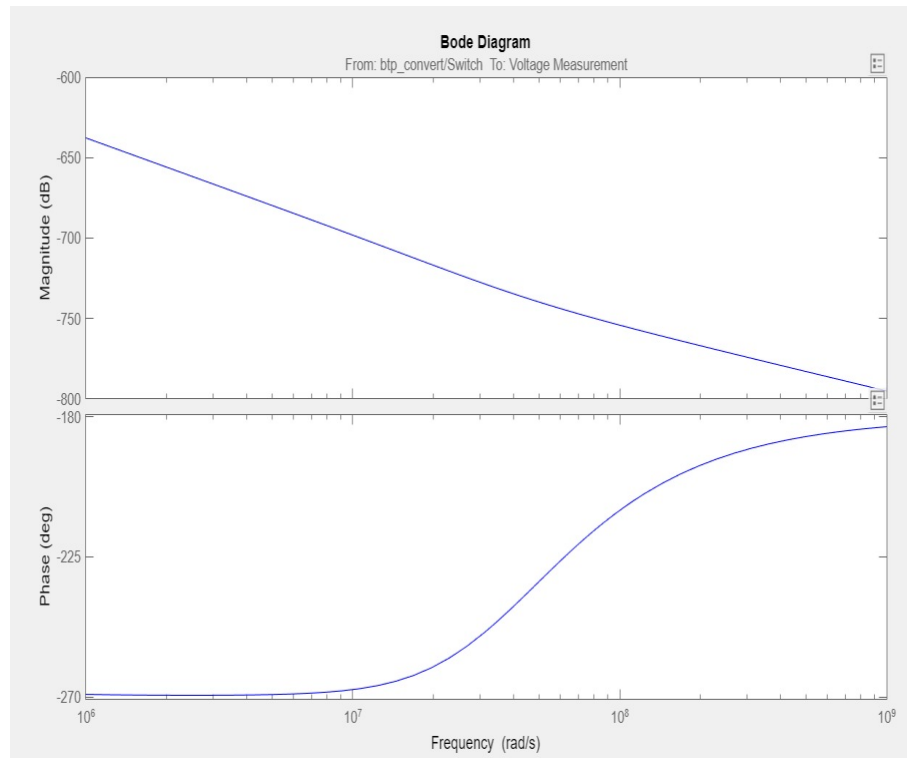


Figure 4.7 Bode plot of control-to-output transfer function in open-loop

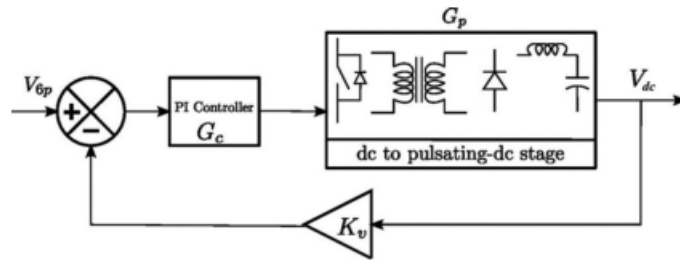


Figure 4.8 Simplified closed-loop block diagram of the dc to pulsating dc stage

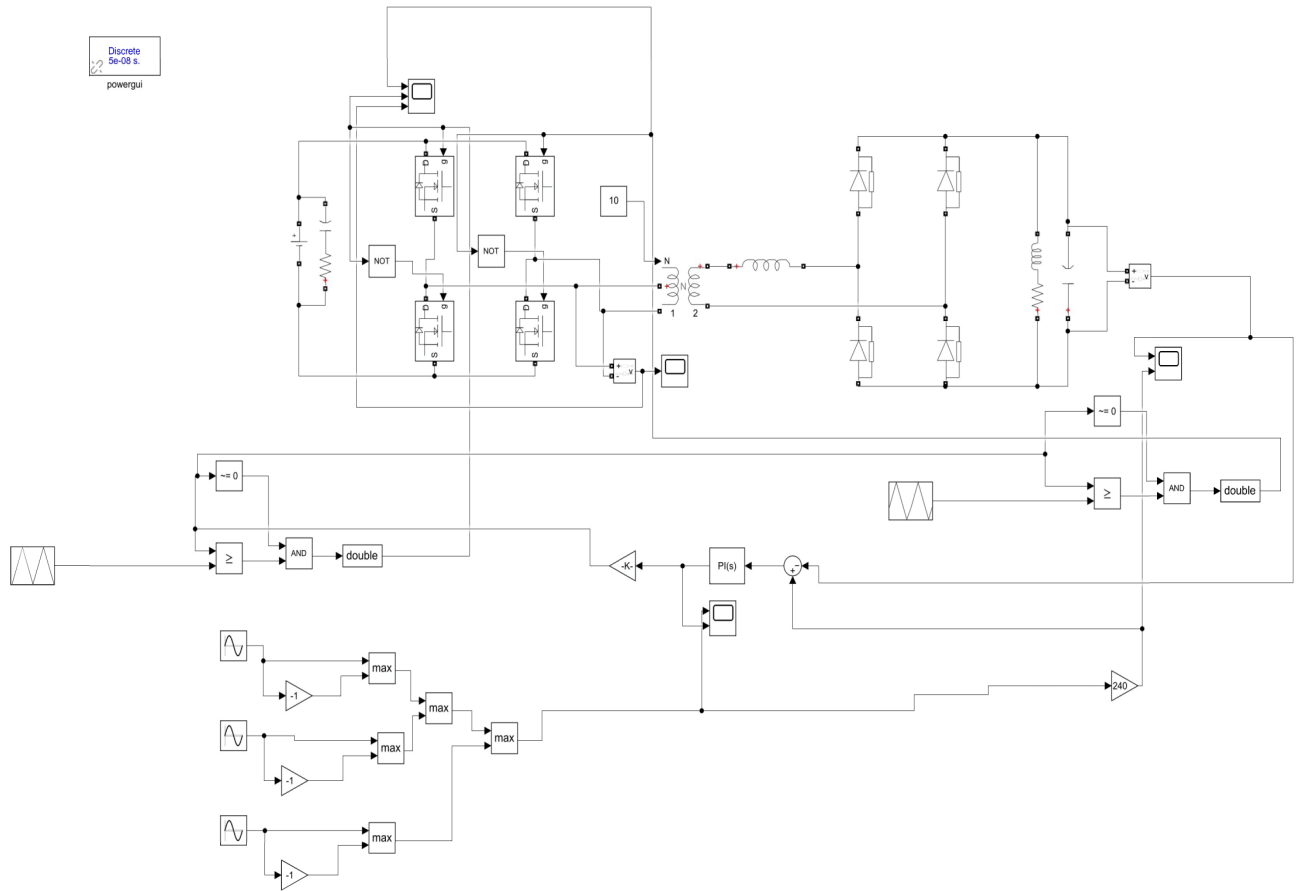


Figure 4.9 Closed-loop Converter Design in MATLAB

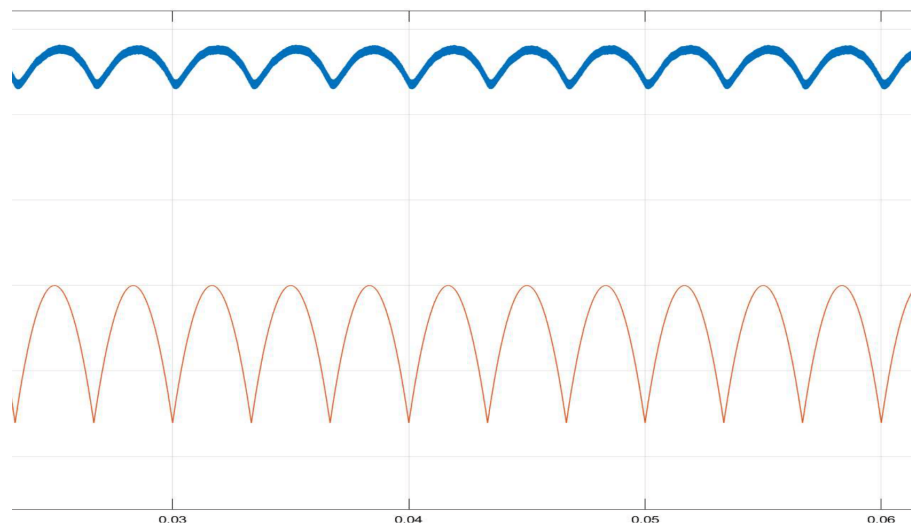


Figure 4.10 Pulsating DC Voltage output of closed-loop control in MATLAB

Chapter 5

Conclusion

The multistage electrolytic capacitor-less inverter's operation is studied. The explanation and experimental demonstration of BCM modes of functioning are done in the project duration. Under step loading conditions, the inverter has been seen to be able to retain the necessary dc bus and its distinctive six-pulse waveform.

The following three major contributions of this research work represented by experimental findings are:

1. Design and implementation of a simple open-loop and closed loop control for the dc bus electrolytic capacitor-less system to obtain three-phase balanced sinusoidal voltage at the output.
2. Understanding the operation of the H-bridge inverter BCM cases.
3. Achieving a 3.4kW power rating and a THD of 3.11% for a dc to three-phase ac converter.

Future Directions

This report gives rise to a number of important tasks and thoughts-

- Hardware implementation of the Closed-loop circuit.
- Reduction of THD.
- 3-Phase Grid Integration and Simulation of hardware.

Bibliography

- [1] X. Pan, A. Ghoshal, Y. Liu, Q. Xu, and A. K. Rathore, “Hybrid-modulation-based bidirectional electrolytic capacitor-less three-phase inverter for fuel cell vehicles: Analysis, design, and experimental results,” *IEEE Transactions on Power Electronics*, vol. 33, no. 5, pp. 4167–4180, 2018.
- [2] H. Haga, K. Nishiya, S. Kondo, and K. Ohishi, “High power factor control of electrolytic capacitor less current-fed single-phase to three-phase power converter,” in *The 2010 International Power Electronics Conference - ECCE ASIA -*, 2010, pp. 443–448.
- [3] U. R. Prasanna and A. K. Rathore, “A novel single-reference six-pulse-modulation (srspm) technique-based interleaved high-frequency three-phase inverter for fuel cell vehicles,” *IEEE Transactions on Power Electronics*, vol. 28, no. 12, pp. 5547–5556, 2013.
- [4] R. Huang and S. K. Mazumder, “A soft switching scheme for multiphase dc/pulsating-dc converter for three-phase high-frequency-link pulsewidth modulation (pwm) inverter,” *IEEE Transactions on Power Electronics*, vol. 25, no. 7, pp. 1761–1774, 2010.
- [5] U. R. Prasanna, A. K. Rathore, and C. Chakraborty, “High-frequency three-phase inverter employing new six-pulse-modulation (spm) technique for rural

- electrification/micro-grid/ders/evs,” in *2013 IEEE International Conference on Industrial Technology (ICIT)*, 2013, pp. 1585–1590.
- [6] A. Ghoshal, X. Pan, and A. K. Rathore, “Analysis and design of closed-loop control of electrolytic capacitor-less six-pulse dc link three-phase inverter,” *IEEE Transactions on Industry Applications*, vol. 53, no. 5, pp. 4957–4964, 2017.
- [7] F. Krismer and J. W. Kolar, “Efficiency-optimized high-current dual active bridge converter for automotive applications,” *IEEE Transactions on Industrial Electronics*, vol. 59, no. 7, pp. 2745–2760, 2012.
- [8] I. Skouros, A. Bampoulas, and A. Karlis, “A bidirectional dual active bridge converter for v2g applications based on dc microgrid,” in *2018 Thirteenth International Conference on Ecological Vehicles and Renewable Energies (EVER)*, 2018, pp. 1–9.
- [9] R. Erickson and D. Maksimovic, *Fundamentals of Power Electronics*, ser. Online access with purchase: Springer. Springer US, 2001. [Online]. Available: <https://books.google.co.in/books?id=On9-rJTR8ygC>